Supporting Information

Nearly Uniform Decaosmium Clusters Supported on MgO: Characterization by X-ray Absorption Spectroscopy and Scanning Transmission Electron Microscopy

Apoorva Kulkarni,[†] Shareghe Mehraeen,[†] Bryan W. Reed,[‡] Norihiko L. Okamoto,[†] Nigel D. Browning,[†,‡] and Bruce C. Gates*[,†]

Department of Chemical Engineering and Materials Science, University of California, One Shields Avenue, Davis, California, 95616, and Condensed Matter and Materials Division, Lawrence Livermore National Laboratory, Livermore, California 94550

Table SI1: Reference Compounds used in EXAFS Contributions

Compound	Absorber-backscatterer pair	*R*(Å)	Type of Reference
Os metal	Os–Os	2.62	Theoretical[a]
$Os_3(CO)_{12}$	Os–C	1.95	Experimental
$Os_3(CO)_{12}$	Os–O*	3.09	Experimental
ReO_2	$Os–O_{support}$	2.10	Theoretical[a]

[a]Theoretical references were generated by FEFF7.

Table SI2: Structural Parameters Corresponding to Structural Model II for EXAFS Data Characterizing the MgO Supported Osmium Species formed by reductive carbonylation of $Os_3(CO)_{12}$ on MgO at 548 K

Model	Absorber–backscatterer pair	*N*	*R* (Å)	$10^3 \times \Delta\sigma^2$ (Å^2)	ΔE_0 (eV)	ε_v^2
Model II	Os–Os	4.5 ± 0.9	2.89 ± 0.02	8.4 ± 2.2	-1.23 ± 1.9	4.9
	Os–C	3.1 ± 0.5	2.60 ± 0.03	3. 3 ± 1.8	3.28 ± 2.3	
	Os–O*	2.1 ± 0.9	3.01 ± 0.02	5.5 ± 3.6	4.56 ± 6.7	
	Os–Mg	1.0 ± 0.3	2.65 ± 0.01	-1.1 ± 2.2	-18.99 ± 8.9	

[a]The errors given in the table correspond to the precisions of the parameters. Notation: *N*, coordination number; *R*, interatomic distance; $\Delta\sigma^2$, Debye-Waller parameter; ΔE_0, inner potential correction; the estimated accuracies of the parameter are as follows: *N*, ±20%; *R*, ±2% Å; $\Delta\sigma^2$, ±20%; ΔE_0, ±20%.

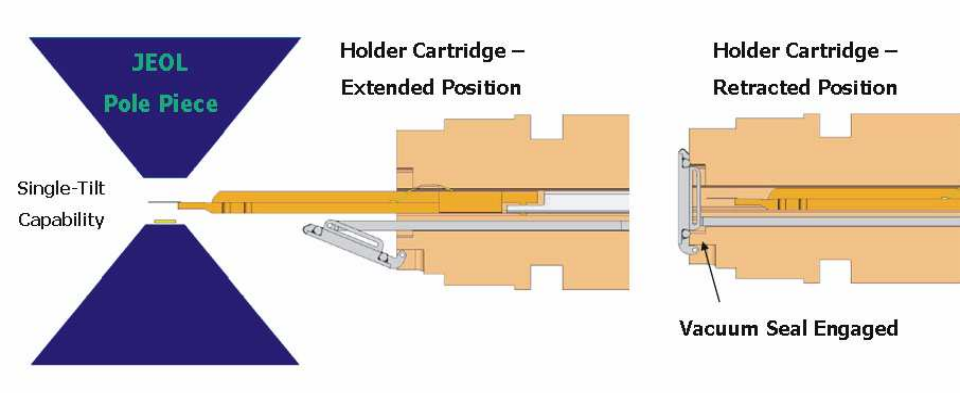

Figure SI 1: Fischione vacuum-transfer-holder (Model 2020).

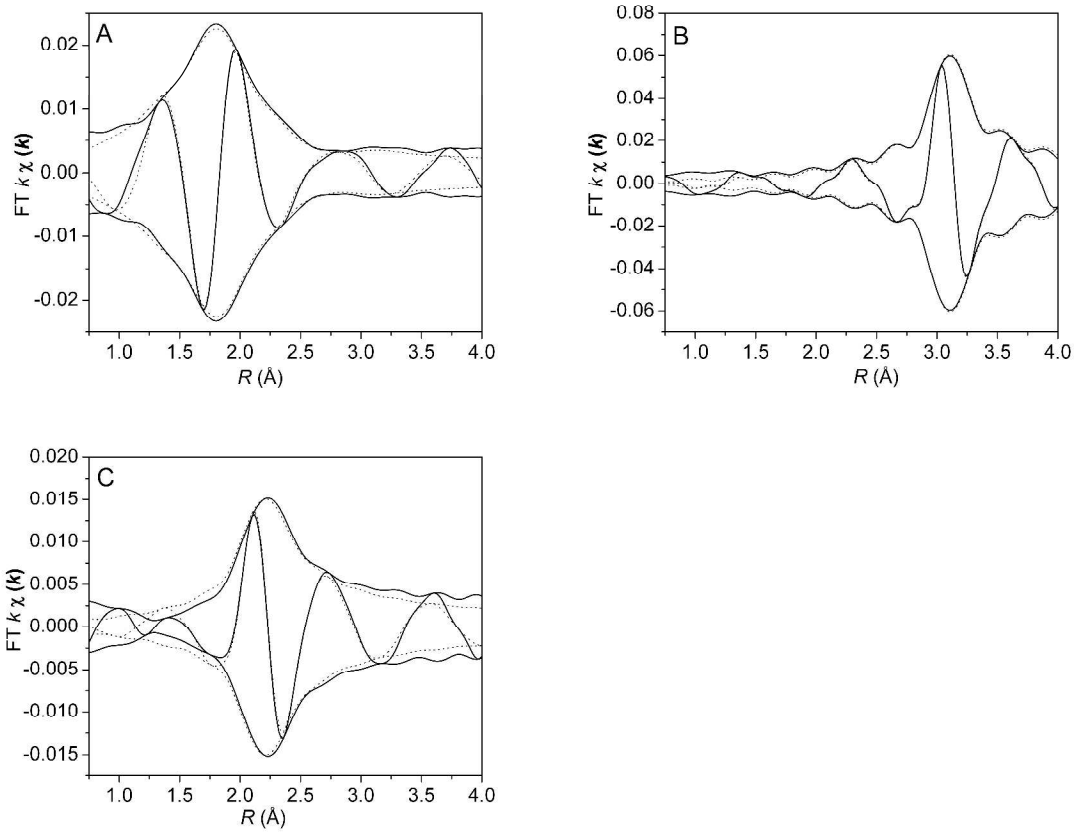

Figure SI 2: EXAFS data (Model I) characterizing species formed by reductive carbonylation of $Os_3(CO)_{12}$ on MgO at 548 K: (A) k^1-weighted, phase corrected, imaginary part and magnitude of the Fourier transform of data (solid line) and calculated contributions (dotted line) of Os–C shell; (B) k^1-weighted, phase corrected, imaginary part and magnitude of the Fourier transform of data (solid line) and calculated contributions (dotted line) of Os–O* shell; (C) k^1-weighted, phase corrected, imaginary part and magnitude of the Fourier transform of data (solid line) and calculated contributions (dotted line) of Os–$O_{support}$ shell.

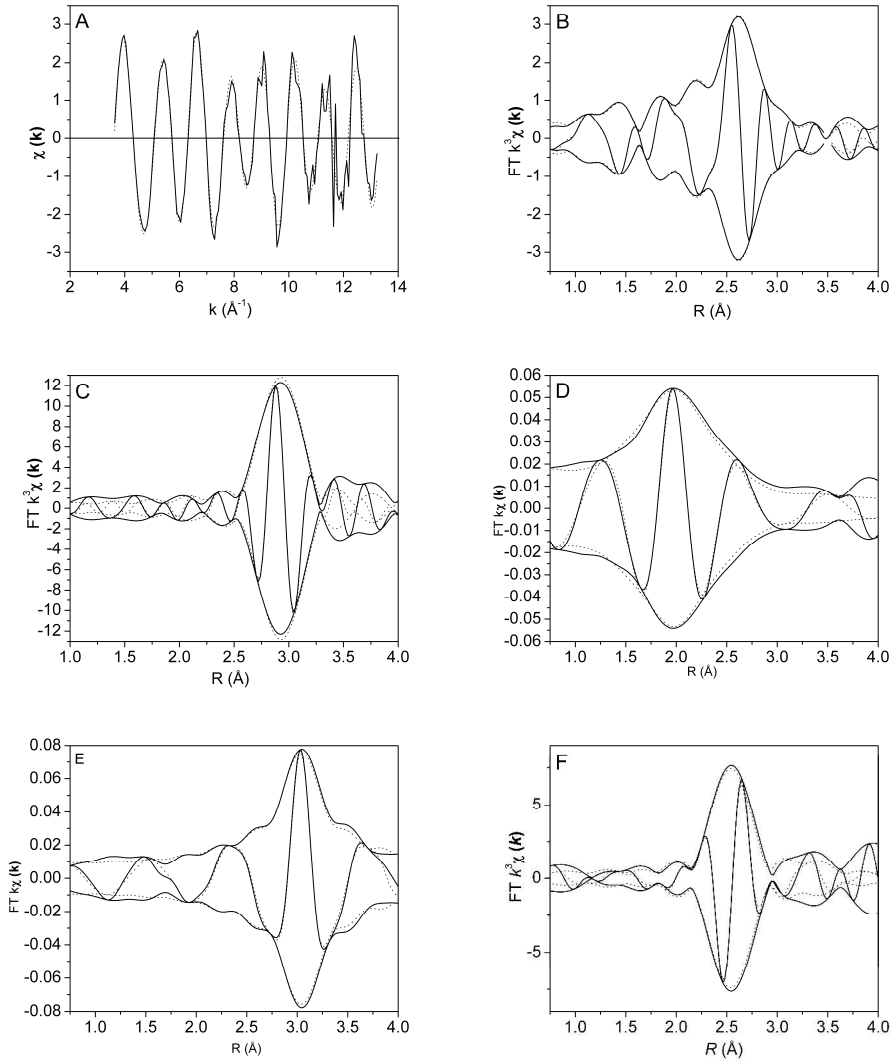

Figure SI 3: EXAFS data (Model II) characterizing species formed from reductive carbonylation of $Os_3(CO)_{12}$ on MgO at 548 K: (A) k^3-weighted EXAFS function, $k^3(\chi)$ (solid line) and sum of the calculated contributions (dotted line); (B) k^3-weighted imaginary part and magnitude of the Fourier transform of data (solid line) and sum of the calculated contributions (dotted line); (C) k^3-weighted, phase and amplitude corrected, imaginary part and magnitude of the Fourier transform of data (solid line) and calculated contributions (dotted line) of Os–Os shell; (D) k^1-weighted, phase corrected, imaginary part and magnitude of the Fourier transform of data (solid line) and calculated contributions (dotted line) of Os–C shell; (E) k^1-weighted, phase corrected, imaginary part and magnitude of the Fourier transform of data (solid line) and calculated contributions (dotted line) of Os–O* shell; (F) k^3-weighted, phase and amplitude corrected, imaginary part and magnitude of the Fourier transform of data (solid line) and calculated contributions (dotted line) of Os–Mg shell.

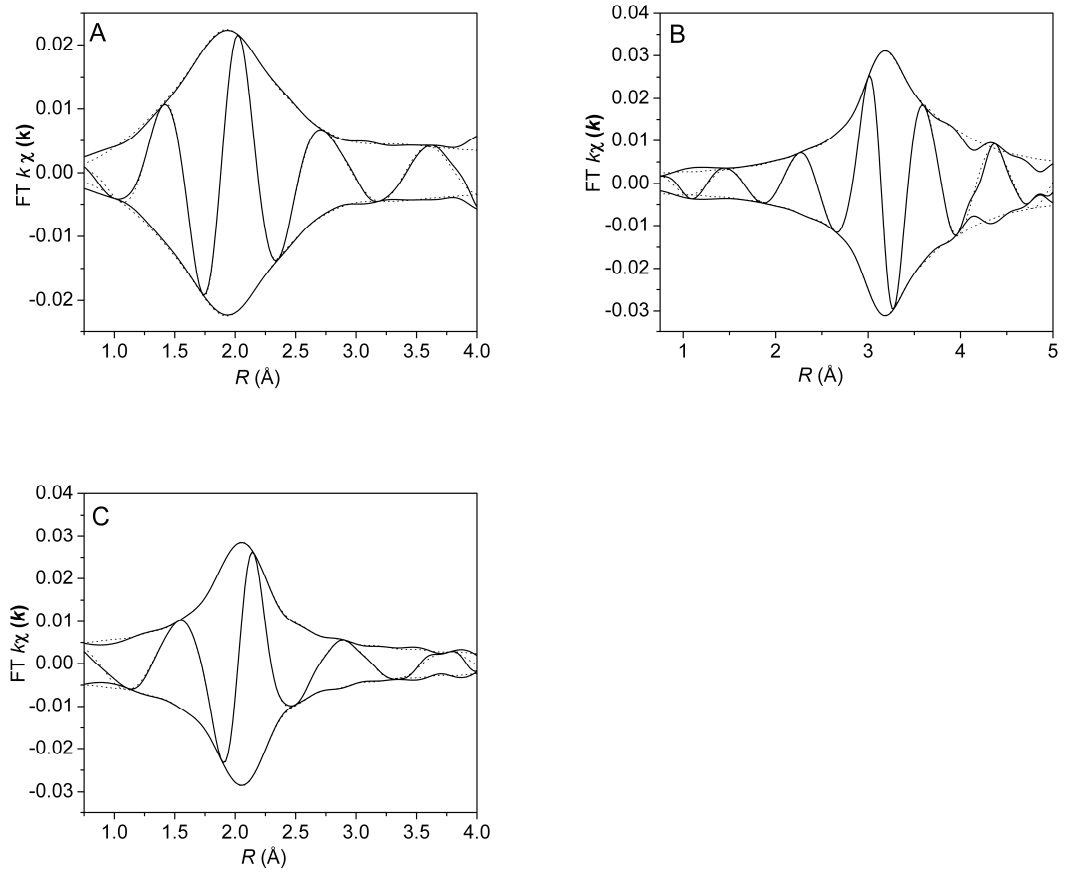

Figure SI 4: EXAFS data (Model III) characterizing species formed by reductive carbonylation of $Os_3(CO)_{12}$ on MgO at 548 K: (A) k^1-weighted, phase corrected, imaginary part and magnitude of the Fourier transform of data (solid line) and calculated contributions (dotted line) of Os–C shell; (B) k^1-weighted, phase corrected, imaginary part and magnitude of the Fourier transform of data (solid line) and calculated contributions (dotted line) of Os–O* shell; (C) k^1-weighted, phase corrected, imaginary part and magnitude of the Fourier transform of data (solid line) and calculated contributions (dotted line) of $Os–O_{support}$ shell.

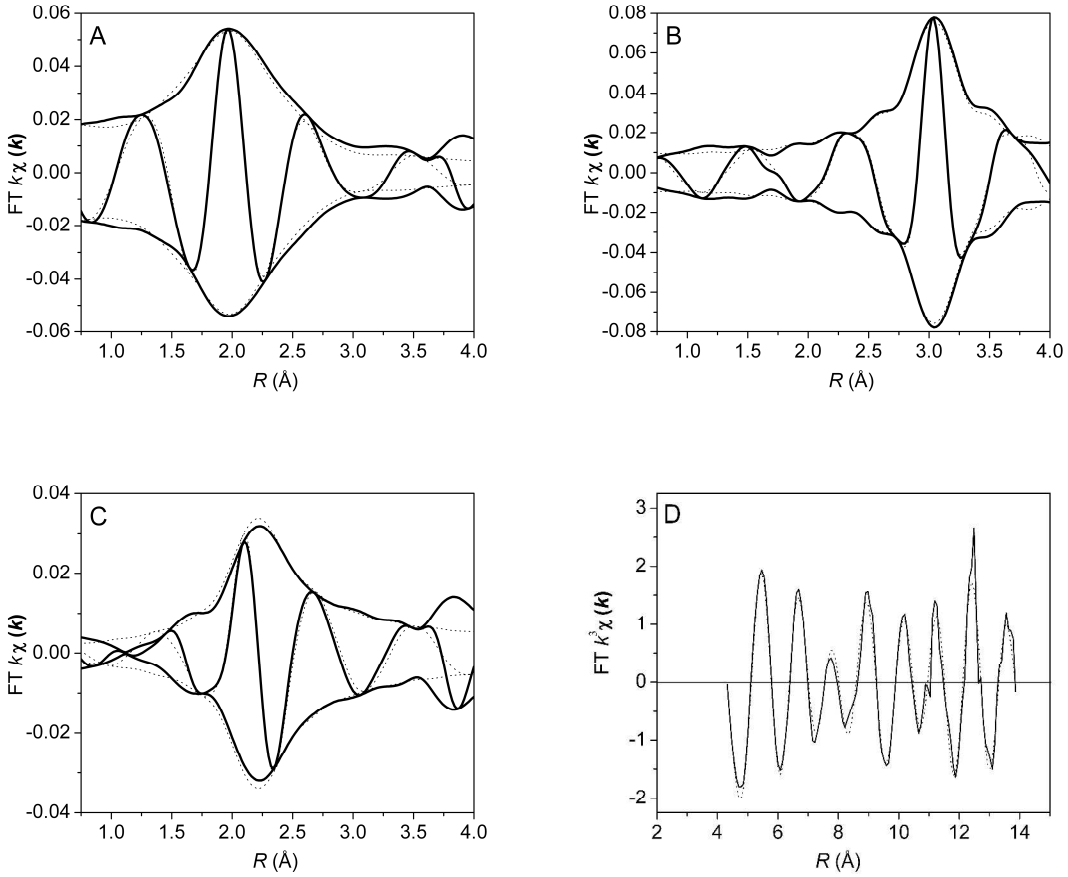

Figure SI 4: EXAFS data (Model IV) characterizing species formed by reductive carbonylation of $Os_3(CO)_{12}$ on MgO at 548 K: (A) k^1-weighted, phase corrected, imaginary part and magnitude of the Fourier transform of data (solid line) and calculated contributions (dotted line) of Os–C shell; (B) k^1-weighted, phase corrected, imaginary part and magnitude of the Fourier transform of data (solid line) and calculated contributions (dotted line) of Os–O* shell; (C) k^1-weighted, phase corrected, imaginary part and magnitude of the Fourier transform of data (solid line) and calculated contributions (dotted line) of Os–$O_{support}$ shell; (D) k^3-weighted EXAFS function, $k^3(\chi)$ (solid line) and sum of the calculated contributions (dotted line).

Example of EXAFS Data Fitting. Described below, as an example, is the detailed analysis carried out for the data characterizing the sample formed by reductive carbonylation of $Os_3(CO)_{12}$ on MgO at 548 K.

The initial data fitting with the plausible absorber–backscatterer contributions (Os–Os, Os–C, Os–Mg, Os-$O_{support}$ and Os–O*, O* and C represent the carbon and oxygen atoms from a carbonyl ligand) led to a narrowed list of to candidate fits (models I and II) on the basis of the goodness of fit. No fit including only a single shell (contribution) was adequate. Both the models found to be most successful in fitting the data included Os−Os contributions. Model I includes two Os–Os contributions, at 2.80 and 2.98 Å, with coordination number of 2.3 and 2.4, respectively, whereas model II included only one contribution, at 2.89 Å, with a coordination number of 4.5. Model I and II each includes contributions from carbonyl ligands, namely, Os–C and Os–O*. All contributions were fitted with reference files that best represent the contributions in the measured sample.

Model I provides the best overall fit, and model II provides a good overall fit as well; however, the shell characterizing the Os−Mg contribution in model II was found not to fit well after the contribution was phase- and amplitude-corrected, showing unrealistic values for ΔE_0 (18.99 ± 8.97 eV). Furthermore, the Debye-Waller factors for the Os−Mg

contribution was < 0, and these values are unrealistic. Of the two models, model I is the one that fits the data better with physically realistic parameters.